Towards Mueller-Tang jets at Next-to-leading order

Federico Deganutti, Timothy Raben, Christophe Royon

The University of Kansas

Low-x Meeting, Bisceglie

fedeganutti@ku.edu

June 14, 2017

Outline

- Motivations and backgrounds
- Mueller-Tang jets at LL
- From LL to NLL
- NLO vet vertex
- Calculation strategy

Physical Motivations

- As was pointed out long ago by Mueller and Tang, the properties of the BFKL hard Pomeron at finite momentum transferred can be investigated at hadron colliders looking for highly exclusive processes where two jets far apart in rapidity represent the sole observed radiation.
- The absence of any additional emission over a large rapidity region suggests that the color-singlet exchange contributes substantially to the jet-gap-jet cross section.

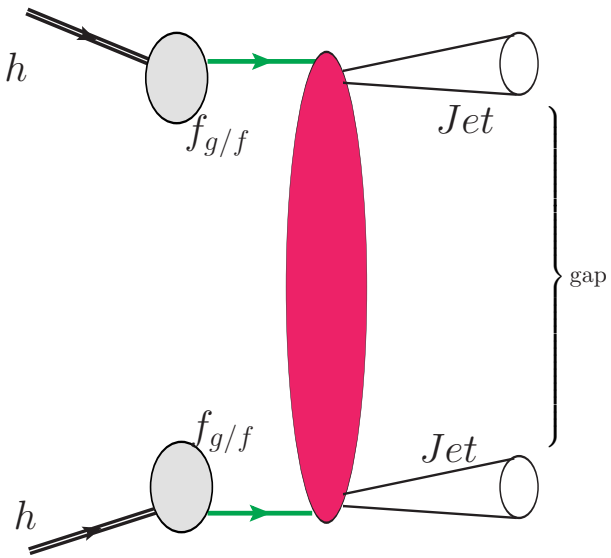

- The BFKL predictions for these processes have been studied at LL accuracy and partially also at NLL order
- The last ingredients that have to be taken into account to complete the approximation order are the NLO impact factors

BFKL description of Mueller-Tang jets

BFKL dynamic effects
are predicted to appear as the rapidity Y between the two jets increases. The imposition of a veto on any other form of radiation favors the description of the interaction thorough the exchange of a color singlet compared to other color representations.

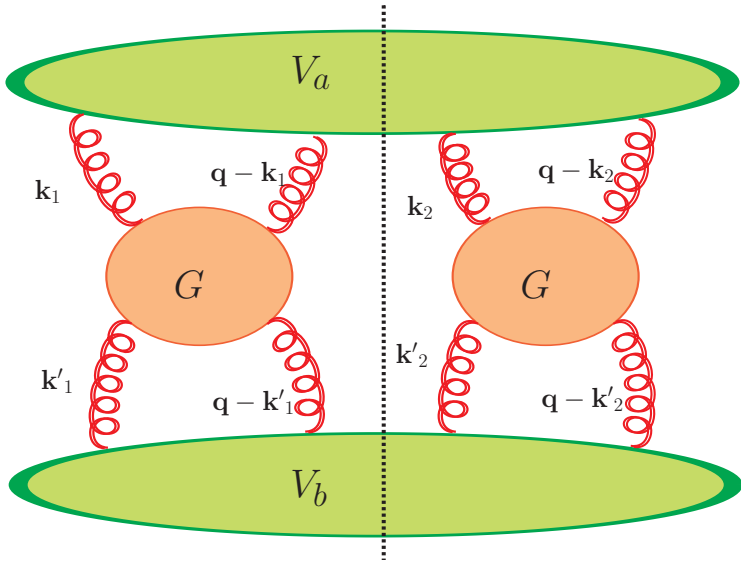

- In general the cross section for these processes is given as a multiple convolution between the the jet vertices and the GGFs.

$$\frac{d\hat{\sigma}}{dJ_1 dJ_2 d^2\mathbf{q}} = \int d^2\mathbf{k}_1 d^2\mathbf{k}'_1 d^2\mathbf{k}_2 d^2\mathbf{k}'_2 V_a(\mathbf{k}_1,\mathbf{k}_2,J_1,\mathbf{q})\times$$
$$G(\mathbf{k}_1,\mathbf{k}'_1,\mathbf{q},Y)G(\mathbf{k}_2,\mathbf{k}'_2,\mathbf{q},Y)V_b(\mathbf{k}'_1,\mathbf{k}'_2,J_2,\mathbf{q}), \qquad J=\{\mathbf{k}_J,x_J\}.$$

- The explicit form of the jet vertex and the Green function depends on the approximation level.

LL approximation: LO vertex

At LL accuracy the Gluon green function G resumms to all orders of perturbation theory the ladder diagrams composed by s-channel gluons connected to t-channel reggeizzed gluons through the Lipatov vertex.

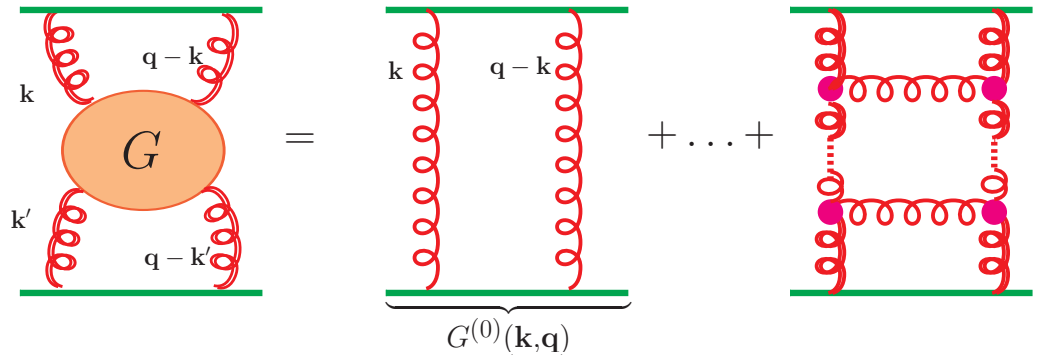

The normalization of the Gluon Green function fixes the jet vertex leading order.

$$\lim_{Y\to 0} G(\mathbf{k},\mathbf{k}',\mathbf{q},Y) = G(\mathbf{k},\mathbf{k}',\mathbf{q},0) = \frac{\delta^2(\mathbf{k}-\mathbf{k}')}{\mathbf{k}^2(\mathbf{q}-\mathbf{k})^2}.$$

At this order, apart for the jet distribution function S that fixes the jet momentum, the jet vertex is a simple color factors (c-number)

$$V_a(x,\mathbf{q},x_J,\mathbf{k}_J) = S_J^0(x,\mathbf{q};x_J,\mathbf{k}_J)h_a^0,$$

$$h_a^0 = C_{q/g}^2\frac{\alpha_s^2}{N_c^2-1}, \qquad S_J^{(0)} = x\delta^2(\mathbf{k}_J-\mathbf{q})\delta(x_J-x).$$

The independence of the LO vertices from the reggeon momenta allow for considerable simplification.

LL approximation: Non forward gluon Green function

The GGF is given by the Mellin transform of the function f_ω which is the solution of the BFKL equation. The solution of the non forward BFKL equation is more naturally expressed in the impact parameter space.

$$G(\mathbf{k},\mathbf{k}',\mathbf{q},Y)=\int_{-i\,\mathrm{inf}}^{+i\,\mathrm{inf}}\frac{d\omega}{2\pi i}e^{Y\omega}f_\omega(\mathbf{k},\mathbf{k}',\mathbf{q})$$

$$f_\omega(\rho_1,\rho_2,\rho_1',\rho_2')=\frac{1}{(2\pi)^6}\sum_{n=-\,\mathrm{inf}}^{+\,\mathrm{inf}}\int_{-\,\mathrm{inf}}^{+inf}d\nu\frac{R_{n\nu}}{\omega-\omega(n,\nu)}E^*_{n\nu}(\rho_1',\rho_2')E_{n\nu}(\rho_1,\rho_2)$$

$$E_{n\nu}(\rho_1,\rho_2)=\underbrace{\left(\frac{\rho_1-\rho_2}{\rho_1\rho_2}\right)^h\left(\frac{\rho_1^*-\rho_2^*}{\rho_1^*\rho_2^*}\right)^{\bar h}}_{\text{Lipatov term}}\quad\underbrace{-\left(\frac{1}{\rho_2}\right)^h\left(\frac{1}{\rho_2^*}\right)^{\bar h}-\left(\frac{-1}{\rho_1}\right)^h\left(\frac{-1}{\rho_1^*}\right)^{\bar h}}_{\text{Mueller-Tang correction}}$$

$E_{n\nu}$ are the eigenfunctions in the impact parameter space.
The GGF in momentum space is recovered applying a Fourier transformation to the eigenfunctions.

$$\tilde E_{n\nu}(\mathbf{k},\mathbf{q})=\int\frac{d^2r_1d^2r_2}{(2\pi)^4}E_{n\nu}(\rho_1,\rho_2)e^{i(\mathbf{k}\cdot\mathbf{r}_1+(\mathbf{q}-\mathbf{k})\cdot\mathbf{r}_2)}$$

Pomeron exchange amplitude

With the leading order vertex independent from the loop momenta the partonic cross section can be expressed as the square modulus of an amplitude that is nothing more than the GGF integrated in its transverse momenta.

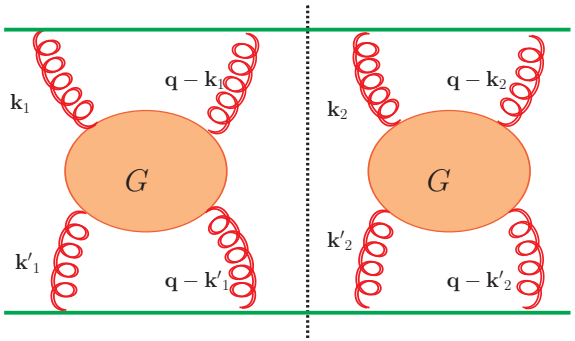

$$A(Y,q) = h_a^0 h_b^0 \int d^2k d^2k' G(\mathbf{k},\mathbf{k}',q,Y), \quad \frac{d\hat{\sigma}}{dq dY} = \frac{1}{16\pi}|A(Y,q)|^2$$

The amplitude can be written in terms of the averaged eigenfunctions $\overline{E}_{n\nu}(\mathbf{q}) = \int d^2k \tilde{E}_{n\nu}(\mathbf{k},\mathbf{q})$. The integration over the transverse momenta greatly simplifies the calculation of the Fourier transform of the eigenfunctions canceling the Lipatov term contribution. The Pomeron exchange amplitude is given by the simple expression

$$A(Y,q) = h_a^0 h_b^0 \sum_{n=-\inf}^{+\inf} \int_{-\inf}^{+inf} d\nu e^{Y\omega_{n\nu}} R_{n\nu}\left(\frac{4}{\mathbf{q}^2}\right)$$

This can be easily extended to include the GGF at NLL $\omega^{LL}(n,\nu) \to \omega^{NLL}(n,\nu)$.

Towards the NL order

The NL impact factors for the Meller-Tang jet process are known[Hentschinski, Madrigal Martinez, Murdaca, Sabio Vera].

Only certain combinations of jet vertex and Gluon Green function approximation orders contribute effectively to the NL order of the cross section. The most complicated combinations can be discarded because they are subleading.

- GGF NLL + LO vertices. For this special case the general formula for the cross section can be expressed in a much simpler form because LL vertices are idependent from the reggeon momenta.
- GGF LL + LO vertex + NLO vertex. The non trivial dependence of the NLO jet vertex from the reggeon momenta introduces an important complication.
- GGF LL + both NLO vertices. Discarded because subleading.

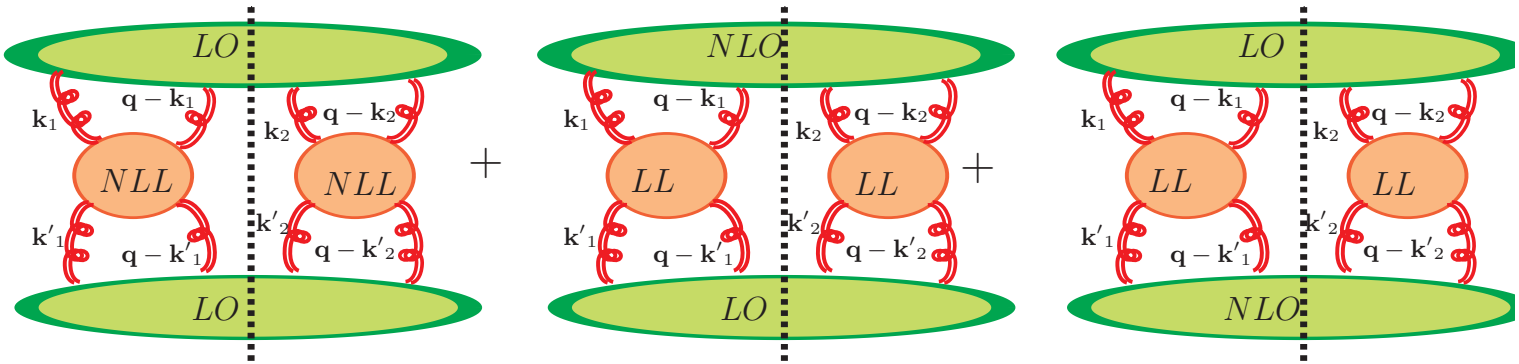

Comparison with experiment

Numerical analysis[Chevalier, Kepka, Marquet, Royon]. Cross sections obtained with HERWIG Monte Carlo program.

Observable definition:

- Ratio $R = \frac{NLL^* BFKL}{NLOQCD}$ of jet-gap-jet events to inclusive dijet events as a function of the transverse momentum of the second-leading jet and the size of the rapidity gap.
- NLL^* BFKL cross section: NLL-BFKL gluon Green function + LO jet vertices (+ collinear resummation).

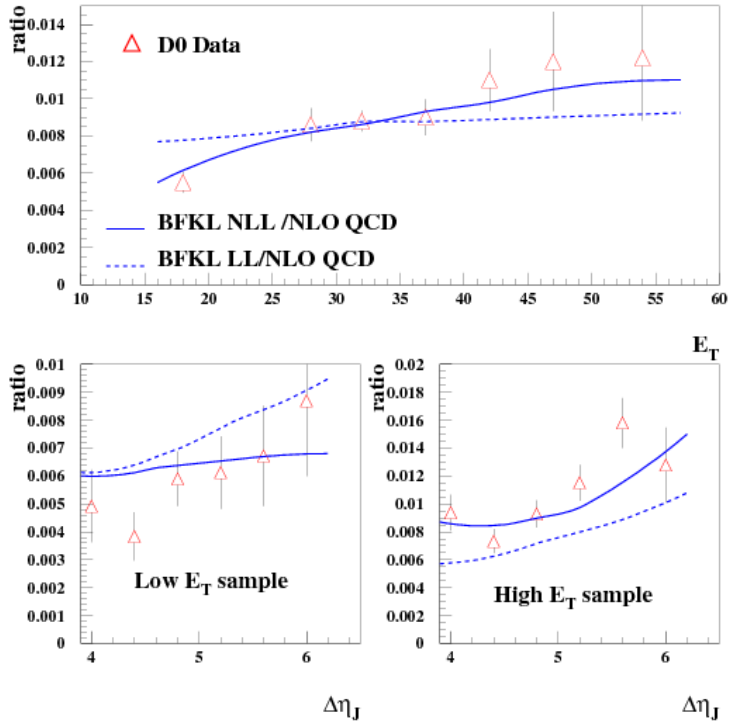

There is a clear preference of the NLL predictions over the LL ones in describing the Tevatron data. The NLL calculation reproduces the experimental data fairly well.

NLO jet vertex

Peculiar characteristics of the NLO the jet vertex.

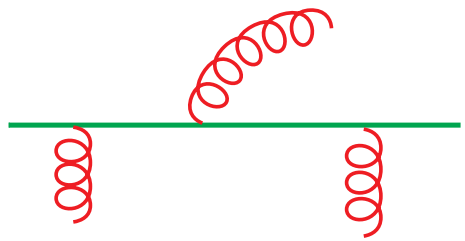

- The non trivial dependence from the reggeon momenta prevents the applicability of the mentioned simplification imposing the use of the general formula.
- Up to two partons can be emitted by the same vertex. Whether they are collinear enough to form the same jet or not depends on the choice of the jet reconstruction algorithm. (1) The two partons form the same jet or (2) one of the two has energy lower than the calorimeter threshold and so it is not detected.
- The soft parton emission in the prohibited region alter the alignment between the forward and the backward jet. The survival of the rapidity gap is assured imposing constraints to the additional parton emission. Jets not back to back anymore $\hat{\sigma}(q, Y) \rightarrow \hat{\sigma}(k_{J_1}, k_{J_2}, \theta_{J_2,J_2}, Y)$

The additional soft emission is needed to assure the cancellation of the infrared divergences.

Numerical analysis

The decision to keep just the pure NL contribution brings some simplification

$$\frac{d\hat{\sigma}}{dJ_1 dJ_2 d^2\mathbf{q}} = \int d^2k_1 d^2k_2 V^1(\mathbf{k}_1, \mathbf{k}_2, \mathbf{q}; J_1) \times \underbrace{\int d^2k'_1 G(\mathbf{k}_1, \mathbf{k}'_1, \mathbf{q}, Y)}_{\overline{G}(\mathbf{k}_1, \mathbf{q}, Y)} \underbrace{\int d^2k'_2 G(\mathbf{k}_2, \mathbf{k}'_2, \mathbf{q}, Y)}_{\overline{G}(\mathbf{k}_2, \mathbf{q}, Y)} V^0(J_2, \mathbf{q})$$

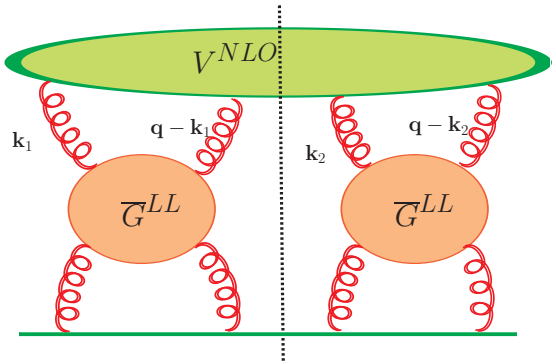

- Large increase in computation time due to the high-dimensional multiple integration.

The full form of the eigenfunction in momentum space is known [Bartels, Braun, Colferai, Vacca].

- The momentum dependence of the eigenfunction is expressed through hypergeometric functions in a region of parameter very sensible to numerical fluctuations. ${}_2F_1(a, b; c, z),\ a - b \in \mathbb{Z}^-$

Numerical analysis

- Calculation of the partonic cross section.
  (1) $\bar{G}$ as a grid of its parameters $\{k_i, q_j, \theta_l, Y_m\}$. It involves a numerical integration over ν and a sum over n for each set of the parameters.
  (2) Partonic cross section as the interpolation of $\bar{G}$ grids and the NLO vertex.

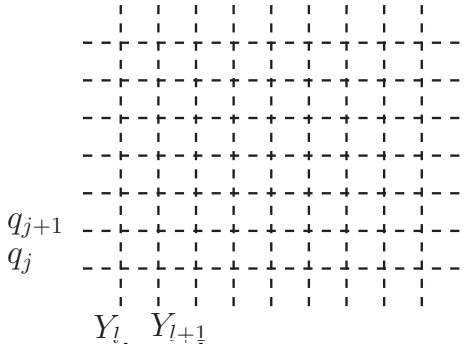

$$\frac{\hat{\sigma}(k_{J_1}, k_{J_2}, \theta_{J_1,J_2}, Y)}{dk_J dY} \propto \sum V(k_{1_i}, k_{2_j}, \theta_{1_n}, \theta_{2_m}, J)\bar{G}(k_{1_i}, q_r, \theta_{1_n}, Y_l)\bar{G}(k_{2_j}, q_r, \theta_{2_m}, Y_l)$$

- Dressing of the initial state and final state hadronization by Herwig
  (1) Proton-proton scattering
  $\frac{d\sigma^{pp\to JGJ}}{dx_1 dx_2 dq} \propto \sum_{a,b} f_a(x_1, k_{J_1}) f_b(x_2, k_{J_2}) \hat{\sigma}(k_{J_1}, k_{J_2}, \theta_{J_1,J_2}, Y)$
  (2) Fitting of the cross section and its substitution by a sum of analytic functions of the fitting parameters.
  (3) Hadronization from the proto-jet to the detector with a matching procedure to remove the double counted diagrams. The error avoided by this subtraction is predicted to be of NL order.

$$\frac{d\hat{V}^{(1)}(x,\boldsymbol{k},\boldsymbol{l}_1,\boldsymbol{l}_2;x_J,\boldsymbol{k}_J;M_{X,\max},s_0)}{dJ} =$$

$$= v_q^{(0)}\frac{\alpha_s}{2\pi}\left[S_J^{(2)}(\boldsymbol{k},x)\cdot\left[-\frac{\beta_0}{4}\left[\left\{\ln\left(\frac{\boldsymbol{l}_1^2}{\mu^2}\right)+\ln\left(\frac{(\boldsymbol{l}_1-\boldsymbol{k})^2}{\mu^2}\right)+\{1\leftrightarrow 2\}\right\}-\frac{20}{3}\right]-8C_f\right.\right.$$

$$+\frac{C_a}{2}\left[\left\{\frac{3}{2\boldsymbol{k}^2}\left\{\boldsymbol{l}_1^2\ln\left(\frac{(\boldsymbol{l}_1-\boldsymbol{k})^2}{\boldsymbol{l}_1^2}\right)+(\boldsymbol{l}_1-\boldsymbol{k})^2\ln\left(\frac{\boldsymbol{l}_1^2}{(\boldsymbol{l}_1-\boldsymbol{k})^2}\right)-4|\boldsymbol{l}_1||\boldsymbol{l}_1-\boldsymbol{k}|\phi_1\sin\phi_1\right\}\right.\right.$$

$$-\frac{3}{2}\left[\ln\left(\frac{\boldsymbol{l}_1^2}{\boldsymbol{k}^2}\right)+\ln\left(\frac{(\boldsymbol{l}_1-\boldsymbol{k})^2}{\boldsymbol{k}^2}\right)\right]-\ln\left(\frac{\boldsymbol{l}_1^2}{\boldsymbol{k}^2}\right)\ln\left(\frac{(\boldsymbol{l}_1-\boldsymbol{k})^2}{s_0}\right)$$

$$\left.\left.-\ln\left(\frac{(\boldsymbol{l}_1-\boldsymbol{k})^2}{\boldsymbol{k}^2}\right)\ln\left(\frac{\boldsymbol{l}_1^2}{s_0}\right)-2\phi_1^2+\{1\leftrightarrow 2\}\right\}+2\pi^2+\frac{14}{3}\right]\Bigg]$$

$$+\ln\frac{\lambda^2}{\mu_F^2}\int_{z_0}^1 dz\; S_J^{(2)}(\boldsymbol{k},zx)\left[P_{qq}(z)+\frac{C_a^2}{C_f^2}P_{gq}(z)\right]$$

$$+\int_0^1 dz\int\frac{d^2\boldsymbol{q}}{\pi}\left[P_{qq}(z)\Theta\left(\hat{M}_{X,\max}^2-\frac{(\boldsymbol{p}-z\boldsymbol{k})^2}{z(1-z)}\right)\Theta\left(\frac{|\boldsymbol{q}|}{1-z}-\lambda\right)\right.$$

$$\times\frac{\boldsymbol{k}^2}{\boldsymbol{q}^2(\boldsymbol{p}-z\boldsymbol{k})^2}S_J^{(3)}(\boldsymbol{p},\boldsymbol{q},(1-z)x,x)$$

$$+\Theta\left(\hat{M}_{X,\max}^2-\frac{\boldsymbol{\Delta}^2}{z(1-z)}\right)S_J^{(3)}(\boldsymbol{p},\boldsymbol{q},zx,x)P_{gq}(z)$$

$$\left.\int C_a\left[\quad\right]+C_a^2\left[\quad\right]\right]$$

$$\tilde{E}_{n\nu}(k_1,k_2) =$$

$$N(n,\nu)\left[{k_1^*}^{\bar{h}-2}{k_2^*}^{h-2}\ {}_2F_1(1-h,2-h;2,-\frac{k_1}{k_2})\ {}_2F_1(1-\bar{h},2-\bar{h};2,-\frac{{k_2^*}^*}{k_1})+\{1\to 2\}\right]$$

$$h=\left(\tfrac{n+1}{2}+i\nu\right),\quad \bar{h}=\left(\tfrac{n-1}{2}-i\nu\right)$$